Theoretical Insights into Effect of Surface Composition of Pt-Ru Bimetallic Catalysts on CH3OH Oxidation: Mechanistic Considerations

Lihui Ou (oulihui666@126.com)
Hunan University of Arts and Science https://orcid.org/0000-0001-5177-2404

Research Article

Keywords: CH3OH oxidation, Pt-Ru alloy, Surface composition, Catalytic activity, Work function

Posted Date: January 14th, 2022

DOI: https://doi.org/10.21203/rs.3.rs-1134900/v1

Abstract

A deeper mechanistic understanding on CH_3OH oxidation on Pt-Ru alloys with different Ru surface compositions is provided by DFT-based theoretical studies in this paper. The present results show that alloying and surface compositions of Ru can change CH_3OH oxidation pathway and activity. The optimal surface composition of Ru is speculated to be *ca*. 50% since the higher Ru surface composition can lead to formation of carbonaceous species that can poison surface. Our present calculated Ru surface composition of *ca*. 50% exhibits excellent consistency with experimental studies. The origin of enhanced catalytic activity of Pt-Ru alloys is determined. The significantly decreased surface work functions after alloying suggest more electrons are transferred into adsorbates. The calculated lower electrode potentials after alloying imply that lower overpotentials are required for CH_3OH oxidation. The excellent inconsistency with experimental study on decreased onset potentials after alloying further confirms accuracy of our present calculated results.

1. Introduction

Direct methanol fuel cells (DMFCs) have attracted extensive attentions and interest as one of the most promising power source in portable applications because of ease of handling of methanol (CH_3OH) and high energy density.[1] At present, Pt as an electrocatalyst can efficiently catalyze CH_3OH oxidation with high kinetics. However, CH_3OH oxidation is facile to be suppressed on pure Pt electrodes by strongly adsorbed CO intermediate, thereby leading to poisoned Pt surface site.[2] Thus, numerous efforts have devoted to seek an effective approach that can alleviate CO poisoning on pure Pt catalyst. Bimetallic Pt-based alloy electrodes may be able to solve this crucial problem. In recent years, considerable research efforts have been made to preparing various bimetallic Pt-based alloy electrocatalysts for use in DFMCs, including Pt-Ru,[3–7] Pt-Fe,[8,9] Pt-Co,[10,11] Pt-Ni,[12–14] Pt-Pd,[15] Pt-Mn,[16] Pt-Sn,[17,18] Pt-Ag,[19,20] Pt-Au,[21–23] and Pt-Mo[24] with higher anti-CO poisoning ability compared to pure electrodes, which have been reported to have positive effects on electrocatalytic stabilities and activities with respect to CH_3OH oxidation. Among these catalysts, the bimetallic Pt-Ru alloys have been recognized to have the best anti-CO poisoning performance and thus partially overcome this challenging problem.

Currently, bimetallic Pt-Ru electrocatalysts are extensively studied in two different forms for CH_3OH oxidation including Pt growth on Ru surface and Pt-Ru alloys with different Pt/Ru surface compositions. A central finding on Pt_n/Ru(0001) surface, namely, the growth of Pt on Ru(0001) is that CH_3OH oxidation pathway is very similar to pure Pt(111) surface and only depends weakly on thickness of the Pt_n/Ru(0001) film.[25–30] Our previous theoretical study also showed that CH_3OH oxidation mechanisms in the presence of sublayer Ru are almost identical with those on pure Pt(111).[31] However, the occurrence of CH_3OH oxidation reaction becomes more difficult for overall optimal pathways in the presence of sublayer Ru than that on pure Pt(111). Thus, it can be speculated that Pt growth on Ru single-crystal surface may not be the optimal way to prepare bimetallic Pt-Ru alloy electrocatalysts, and the Pt-Ru

alloys with different Ru surface compositions may be proper for CH_3OH electrooxidation. In fact, the previous experimental studies showed that bimetallic Pt-Ru alloys had larger CO_2 yield during CH_3OH oxidation than that on Pt_n/Ru(0001). For example, the results from Corti et al. indicated that Pt-Ru alloy electrocatalysts with more than 15% Ru surface compositions can lead to slightly decreased values of poisoning rate,[32] in which the presence of Ru may be able to prevent poisoning of Pt surface active sites. Furthermore, the change of equilibrium potential is observed as increasing Ru surface compositions, indicating a change in the rate-determining step. The experimental investigations on CH_3OH oxidation conducted by Iwasita et al. showed that the activity of Pt-Ru alloys in the range from 10–40% of Ru surface composition is up to a factor of 10 higher than that of pure Pt(111) and other Pt-based alloys.[33–35] The model proposed by Ross et al. indicated that a surface structure having one Ru atom neighboring three Pt sites may be able to represent the optimum geometry for CH_3OH oxidation, namely, 25% of Ru surface composition.[36] A *ca*. 50% of Ru surface composition was deemed to be able to achieve the best electrocatalytic activity for CH_3OH oxidation and anti-CO poisoning ability in early experiments from Gasteiger et al., Weidner et al. and Wei et al.[37–40] Although it has been well known that alloying Pt with Ru with approximate Ru surface compositions can notably enhance CH_3OH oxidation activity for decades, mechanistic understandings on origin of enhanced electrocatalytic activity at the atomic scale are still elusive.

Presently, it is generally accepted that a bifunctional mechanism of bimetallic Pt-Ru alloy catalysts be responsible for enhanced electrocatalytic activity during CH_3OH oxidation,[37, 38, 41] in which surface Pt sites are required for adsorption and oxidation of CH_3OH and effective dissociation of H_2O molecules into oxygen-containing species occurs at lower electrode potentials on adjacent surface Ru sites compared with pure Pt surface that can remove oxidative intermediates like CO produced by CH_3OH dehydrogenation. For example, the onset of CH_3OH oxidation is *ca*. 450 mV on pure Pt electrodes by cyclic voltammetry, whereas which is decreased into *ca*. 250 mV on Pt-Ru alloy electrocatalysts. The differential electrochemical mass spectrometry (DEMS) can be facile to verify this phenomenon by detecting the onset of CO_2 production at the respective potentials.[42] Thus, it is concluded that CO poisoning can be alleviated by oxidizing strongly adsorbed CO intermediate into CO_2 on Pt-Ru alloys.[37] The origin of enhanced electrocatalytic activity in the bifunctional mechanisms may be able to be ascribed to the change of electronic structures of Pt when the more electronegative Ru is alloyed.[43–45] However, apart from the indirect pathways that can form CO intermediate during CH_3OH oxidation, a dual path mechanism may occur on bimetallic Pt-Ru alloys,[42, 46–48] in which direct pathways may exist, proceeding via oxidation of HCOOH intermediate to form CO_2. For example, HCOOH species had been detected in DEMS experiments from Vielstich et al. by monitoring the signal of methylformate,[42] suggesting that the excellent anti-CO poisoning ability of bimetallic Pt-Ru alloys may be not easier removal of CO intermediate, but change of oxidation pathways of CH_3OH. Using in situ Fourier transform infrared-diffuse reflection analysis, the most recent experimental study from Wei et al. indicated that reaction intermediates of CH_3OH oxidation can be controlled by manipulating the surface compositions

of Pt-Ru alloys,[40] in which CH_3OH oxidation reaction proceed via $HCOO^-$ intermediate on the Pt-Ru alloy surfaces with rich Pt, whereas the pathways via CO intermediate is more favorable on the Ru-rich Pt-Ru alloy electrocatalysts. Although the above experimental studies provided some valuable mechanistic information about origin of enhanced electrocatalytic activity, some controversies still exist, and little is known about reaction intermediates included in CH_3OH oxidation mechanism on Pt-Ru alloys. Therefore, it is indispensable to achieve mechanistic understanding on CH_3OH oxidation on Pt-Ru alloy catalyst surfaces, especially effect of surface composition of Ru on CH_3OH oxidation pathways, which will help to rationally design cost-effective and sustainable Pt-based alloy electrocatalysts for DMFCs.

A deeper understanding on CH_3OH oxidation mechanisms on Pt-Ru alloys with different Ru surface compositions may be able to be provided by density functional theory (DFT)-base theoretical studies. However, previous DFT work only devoted to theoretical insights into CH_3OH oxidation mechanisms on pure Pt surface.[49–51] Furthermore, only indirect pathway that proceeded via CO intermediate was studied, and direct pathway included HCOOH species seemed to be ignored on pure Pt surface. To our knowledge, no relevant theoretical studies for the effect of Ru surface compositions in Pt-Ru alloys on CH_3OH oxidation mechanisms have been reported at present, especially, the effect of Ru surface composition on catalytic activity. Accordingly, many crucial questions are still ambiguous for CH_3OH oxidation on Pt-Ru alloy catalysts with different Ru surface compositions. For instance, which bond is initially broken during CH_3OH oxidation, C-O, C-H or O-H? What are the reaction intermediates and rate-determining steps? How do Ru surface compositions influence CH_3OH oxidation pathways? What is the optimum Ru surface composition for CH_3OH oxidation? A systematic understanding of the atomic- and molecular-level processes on CH_3OH oxidation mechanisms on Pt-Ru alloy catalysts with different Ru surface compositions will result in the ultimate goal of the explanation of origin of enhanced electrocatalytic activity and design of electrocatalysts. Thus, we perform a systematic DFT study on CH_3OH oxidation pathway on Pt-Ru(111) alloy catalysts, and present a detailed potential energy surface showing the interconversions of the various intermediates. It is hoped that theoretical insights that obtained in present paper will eventually result in the development of improved DMFC anode electrocatalysts.

2. Results And Discussion

2.1 CH_3OH oxidation pathways on pure Pt(111) surface

Surface and solvation models and computational details are given in Supporting Information. For comparison, CH_3OH electrooxidation mechanisms on pure Pt(111) surface in aqueous phase that calculated in our previous work are sketched out to examine the effect of alloying in this paper.[31] As can be seen in Figure 1 (a), our previous DFT calculated results indicate that the optimal indirect pathway of CH_3OH electrooxidation into CO_2 mainly occurs by initialing with C-H bond scission via intermediates CH_2OH, CHOH, CHO and CO on pure Pt(111) surface in aqueous phase, in which COH species may be only a spectator. The oxidation rate may be able to be determined by C-H bond cleavage of CH_2OH into

CHOH intermediate and CO further oxidation into CO_2 due to their relatively higher activation barriers. The direct pathways may occur through CHO hydroxylation into HCOOH intermediate and its further oxidation to form CO_2, as shown in Figure 1(b). Combined with CHO formation and its further oxidation into CO_2, the optimal direct pathway possibly takes place through intermediates CH_2OH, CHOH, CHO, HCOOH, HCOO, and COOH on pure Pt(111) surface, in which the rate-determining step is C-H bond cleavage of CH_2OH into CHOH species. By comparing formation barrier of CO intermediate with that of HCOOH species during CHO further oxidation (*ca*. 0.28 eV *vs*. 0.10 eV), it is found that both are very low and surmountable at room temperature, suggesting that the indirect and direct pathways may be able to parallelly occur on pure Pt(111) surface. However, a high barrier of *ca*. 0.88 eV is required for CO further oxidation to CO_2 product, which can lead to poisoning of surface Pt active sites due to adsorbed CO, explaining why CH_3OH electrooxidation experimentally is facile to be suppressed on pure Pt electrodes. The corresponding energetics for possible elementary reaction steps involved in indirect and direct pathways on pure Pt(111) surface in aqueous phase are summarized in Table S1.

2.2 CH_3OH oxidation pathways on Pt-Ru alloy surfaces

The optimized structures for various possible adsorbed species on Pt-Ru alloys with different Ru surface compositions are given in Figures S1-3, which are employed to carry out MEP analyses. Formation pathways of key intermediate CO are firstly examined initial with C-H, O-H and C-O bond scissions of CH_3OH in this paper. As can be seen in Figures 2 and 3, the activation barriers for C-H bond cleavage to form the adsorbed CH_2OH species are calculated as *ca*. 0.67, 0.27 and 0.28 eV with energy change of reaction of *ca*. -0.01, -0.16 and -0.35 eV on $Pt_2Ru(111)$, PtRu(111) and $PtRu_2(111)$, respectively. For formation of adsorbed CH_3O species via O-H bond breakage, the calculated barriers are *ca*. 1.15, 1.11 and 0.58 eV with reaction energies of *ca*. 0.72, 0.63 and -0.27 eV, respectively. For C-O bond cleavage into the adsorbed CH_3 species, the barriers are calculated as *ca*. 1.50, 1.58 and 0.38 eV with energy change of reaction of *ca*. 0.50, -0.20 and -0.42 eV, respectively. The above MEP analyses indicate that initial CH_3OH oxidation into CH_2OH species via C-H bond scission may be the most favorable on Pt-Ru alloys due to significantly lower barriers and more exothermic or less endothermic than those of O-H and C-O bond breakage, which are well agreeable with previous theoretical homogeneous dehydrogenation studies in aqueous phase on pure Pt(111) surface from us, Mattsson et al. and Okamoto et al.[31, 52, 53] Thus, only the oxidation pathway that initial with C-H bond breakage of CH_3OH is further considered on Pt-Ru alloys with different Ru surface compositions in aqueous phase.

Beginning with further CH_2OH oxidation, two possibilities are considered. An activation barrier of *ca*. 0.42, 0.15 and 0.38 eV is required for C-H bond scission to form CHOH species on $Pt_2Ru(111)$, PtRu(111) and $PtRu_2(111)$ with the reaction energies of *ca*. 0.30, -0.43 and -0.73 eV, respectively, whereas formation of CH_2O species via O-H bond scission need to overcome the barrier of *ca*. 0.94, 0.73 and 0.34 eV with energy change of reaction of *ca*. 0.87, 0.46 and -0.40 eV, respectively. We find that CH_2OH intermediate can be facile to further oxidize to form the adsorbed CHOH intermediate via C-H bond activation step on

$Pt_2Ru(111)$ and $PtRu(111)$, as demonstrated by significantly lower barrier and more exothermic values of reaction energies compared to those of O-H bond cleavage to form adsorbed CH_2O species. However, CH_2OH intermediate further oxidizes through C-H and O-H bond activation steps to form the adsorbed CHOH and CH_2O intermediates both have low and approximately equal activation barriers with exothermic values of reaction energies on $PtRu_2(111)$, suggesting that CHOH and CH_2O intermediates may be able to be simultaneously formed and both pathways may be able to parallelly occur on $PtRu_2(111)$.

The adsorbed CHO or COH species may be able to be further formed by either O-H or C-H bond breakage steps of CHOH species formed by CH_2OH oxidation. The calculated barrier is *ca*. 0.50, 0.43 and 0.26 eV for O-H bond scission into CHO species with reaction energies of *ca*. 0.32, 0.20 and -0.44 eV on $Pt_2Ru(111)$, $PtRu(111)$ and $PtRu_2(111)$, respectively. C-H bond cleavage to COH requires the barriers of *ca*. 0.16, 0.03 and 0.03 eV, respectively. The corresponding reaction energies are *ca*. -0.19, -0.48 and -1.28 eV. It can be found that significantly lower barriers are required for COH formation than that of CHO on $Pt_2Ru(111)$, $PtRu(111)$ and $PtRu_2(111)$, which are almost non-activated processes with exothermicity and can be overcome at room temperature, suggesting that C-H bond breakage into COH may be more facile to occur. However, we also observe that CHO formation barrier is also very low and can be easily overcome with exothermicity on $PtRu_2(111)$, suggesting that O-H bond scission in CHOH species is also possibly to occur. The produced CH_2O by CH_2OH oxidation can also react via C-H bond cleavage step to form adsorbed CHO on $PtRu_2(111)$. The required barrier is extremely low (0.10 eV) with a exothermic reaction energy of -0.47 eV. Thus, the results showed that CHO can be facile to form through CHOH and CH_2O further oxidation, which maybe parallel pathways on $PtRu_2(111)$.

Table 1 Activation barriers (E_{act}, eV) and reaction energies (E_{reac}, eV) for possible elementary reaction steps involved during CH_3OH oxidation into CO on $Pt_2Ru(111)$, $PtRu(111)$ and $PtRu_2(111)$

Elementary Reaction Steps	$Pt_2Ru(111)$		$PtRu(111)$		$PtRu_2(111)$	
	E_{act}, eV	E_{reac}, eV	E_{act}, eV	E_{reac}, eV	E_{act}, eV	E_{reac}, eV
$CH_3OH^* \rightarrow CH_2OH^* + (H^+ + e^-)$	0.67	-0.01	0.27	-0.16	0.28	-0.35
$CH_3OH^* \rightarrow CH_3O^* + (H^+ + e^-)$	1.15	0.72	1.11	0.63	0.58	-0.27
$CH_3OH^* \rightarrow (CH_3 + OH)^*$	1.50	0.50	1.58	-0.20	0.38	-0.42
$CH_2OH^* \rightarrow CHOH^* + (H^+ + e^-)$	0.42	0.30	0.15	-0.43	0.38	-0.73
$CH_2OH^* \rightarrow CH_2O^* + (H^+ + e^-)$	0.94	0.87	0.73	0.46	0.34	-0.40
$CHOH^* \rightarrow CHO^* + (H^+ + e^-)$	0.50	0.32	0.43	0.20	0.30	-0.44
$CHOH^* \rightarrow COH^* + (H^+ + e^-)$	0.16	-0.19	0.03	-0.48	0.03	-1.28
$CH_2O^* \rightarrow CHO^* + (H^+ + e^-)$	\	\	\	\	0.10	-0.47
$CHO^* \rightarrow CO^* + (H^+ + e^-)$	\	\	\	\	0.02	-1.03
$COH^* \rightarrow CO^* + (H^+ + e^-)$	0.08	-0.64	0.39	-0.39	0.16	-0.67
$(CO + OH)^* \rightarrow CO_2^* + (H^+ + e^-)$	0.68	0.11	0.68	0.72	1.21	0.84

The further oxidation of adsorbed COH species to form key intermediate CO need to overcome barriers of *ca*. 0.08, 0.39 and 0.16 eV with negative reaction energies of *ca*. -0.64, -0.39 and -0.67 eV on $Pt_2Ru(111)$, $PtRu(111)$ and $PtRu_2(111)$, respectively. Conversion of adsorbed CHO produced by CH_2O species to form stable adsorbed CO requires a barrier of *ca*. 0.02 eV with strong exothermicity of *ca*. -1.03 eV on $PtRu_2(111)$. The results show that intermediate CO can produced by COH further oxidation on $Pt_2Ru(111)$, $PtRu(111)$ and $PtRu_2(111)$ and CHO further oxidation on $PtRu_2(111)$ due to the surmountable barriers at room temperature, as shown in Figures 2 and 3. The corresponding energetics for possible elementary reaction steps involved during CH_3OH oxidation into CO on Pt-Ru alloys with different Ru surface compositions are summarized in Table 1.

In indirect pathway, the formed key intermediate CO further oxidation can lead to production of CO_2 product. The corresponding activation barrier is *ca*. 0.68, 0.90 and 1.21 eV on $Pt_2Ru(111)$, $PtRu(111)$ and $PtRu_2(111)$ with the reaction energy of *ca*. 0.11, 0.72 and 0.84 eV (See Table 1), respectively. Our present proposed optimal CH_3OH oxidation pathways to produce CO_2 products on Pt-Ru(111) alloys with different Ru surface compositions initial with C-H bond scission are given in Figure 4. As is well-known, CHO species, as a generally accepted reactive intermediate in indirect and direct pathways for CH_3OH oxidation, may be able to lead to formation of HCOOH intermediate in the direct pathway via

hydroxylation. And then, the final production CO_2 can be produced via successive oxidation of HCOOH. Formation of CHO species is unfavorable on $Pt_2Ru(111)$ and PtRu(111) due to significantly higher barriers than those of COH (See Table 1), suggesting that the direct pathways via HCOOH intermediate is impossible to occur. Formation pathways of CHO and COH species may be able to parallelly occur on $PtRu_2(111)$ due to the low and almost identical barriers. Thus, it can be speculated that the direct pathways via HCOOH intermediate may be able to occur on $PtRu_2(111)$. However, an extremely high barrier of *ca*. 1.50 eV is required for CHO hydroxylation into HCOOH with strong endothermic process of *ca*. 1.31 eV, suggesting that the direct pathway is also difficult to occur and CHO species only can lead to CO formation on $PtRu_2(111)$. The most recent experimental study from Wei et al. also showed that the pathways via CO intermediate is more favorable on the Ru-rich Pt-Ru alloy electrocatalysts,[40] further validating accuracy of our present theoretical studies.

2.3 Effect of Ru surface composition on CH_3OH oxidation pathways

As above elaborated, the indirect pathways through CHO and CO intermediates and direct pathways via HCOOH intermediate may be able to parallelly occur on pure Pt(111) surface, as shown in Figure 4(a). After alloying of Pt with Ru, only indirect pathways occur due to difficult formation of HCOOH species, as can be seen in Figure 4 (b) and (c). Thereinto, formation of COH species is more favorable than CHO on $Pt_2Ru(111)$ and PtRu(111), whereas COH and CHO species may be able to simultaneously form on $PtRu_2(111)$ with higher Ru surface compositions. Thus, the changes of Ru surface compositions may be able to lead to different CH_3OH oxidation pathways. In the mean time, it is noted that barriers of some elementary steps during CH_3OH oxidation into CO are significantly decreased after alloying of Pt with Ru compared with those of pure Pt surface. C-H bond scission into CH_2OH species is the optimal initial CH_3OH oxidation pathway on pure Pt(111) and Pt-Ru alloys. The corresponding barrier is *ca*. 0.80 eV on pure Pt(111). We observe that CH_2OH formations barrier is reduced into *ca*. 0.67 eV when surface composition of Ru is *ca*. 33%, and it has approximately equal and the lowest value of barrier (*ca*. 0.28 eV) when surface composition of Ru is *ca*. 50% and 67%. The most recent experimental results from Wei et al. observed a higher forward peak current for C-H bond scission of CH_3OH when surface composition of Ru is *ca*. 50%, indicating a faster kinetic rate and confirming our present theoretical results.[40] CH_2OH further oxidation inclines to form CHOH intermediate on pure Pt(111) surface and when surface composition of Ru is *ca*. 33% and 50%, in which CHOH formation barrier is significantly decreased into *ca*. 0.42 and 0.15 eV as increasing Ru surface compositions compared with that of pure Pt(111) surface (*ca*. 0.95 eV). However, intermediates CHOH and CH_2O may be able to be simultaneously formed during CH_2OH further oxidation due to very low and almost equal activation barriers (*ca*. 0.38 eV *vs*. 0.34 eV) when Ru surface composition is increased into *ca*. 67%, which are also notably lower than that of pure Pt(111) surface. It can be observed that CH_2OH further oxidation into CHOH species has lowest barrier when surface composition of Ru is *ca*. 50%, suggesting that surface compositions of more than 50% will be not favor of CH_2OH oxidation.

CHOH further oxidation into CHO and COH species both are facile to occur on pure Pt(111) surface, which have extremely low and almost equal barriers (*ca*. 0.10 eV) and are almost non-activated processes. However, the barrier is notably increased for CHOH further oxidation into CHO species after alloying of Pt with Ru compared with that of pure Pt(111) surface. CHOH further oxidation into COH species through C-H bond scission is relatively more easily to occur than O-H bond scission into CHO. COH formations are all almost non-activated processes due to extremely low barriers (*ca*. 0.10 eV) on Pt-Ru alloys with different Ru surface compositions. Moreover, increasing Ru surface compositions make COH formation barriers reduce into below 0.10 eV, namely, COH formations have the lowest values, *ca*. 0.03 eV when surface composition of Ru is *ca*. 50% and 67%, being slightly lower than those of pure Pt(111) surface. Simultaneously, we also noted that CHO is also possibly to be formed by CH_2O further oxidation due to very low barrier (*ca*. 0.10 eV) when surface composition of Ru is *ca*. 67%. After alloying of Pt with Ru, the required barriers for COH and CHO further oxidation into key intermediate CO are also significantly reduced compared with that of pure Pt(111) surface. Thereinto, CO is formed mainly by COH further oxidation with the surmountable barriers at room temperature when surface composition of Ru is *ca*. 33%, 50% and 67% and CHO further oxidation into CO is also possibly to occur with extremely low barrier (*ca*. 0.02 eV) when surface composition of Ru is *ca*. 67%. CO further oxidation can lead production of final CO_2 product via hydroxylation, in which OH may be from dissociation of H_2O molecule in aqueous phase. The required barrier is reduced to *ca*. 0.68 eV when surface composition of Ru is *ca*. 33% compared with that of pure Pt(111) surface (*ca*. 0.88 eV), as shown in Figure 5(a). The almost identical barrier is observed (*ca*. 0.90 eV) with that of pure Pt(111) surface when surface composition of Ru is *ca*. 50%. Ru surface composition of *ca*. 67% make the barrier notably increase into *ca*. 1.21 eV. The increasing barrier as increasing Ru surface compositions may be able to be attributed to the increasing barrier for H_2O dissociation into adsorbed OH species, as shown in Figure 5(b), which is an essential intermediate for CO hydroxylation in indirect pathway. Furthermore, higher oxygen affinity of Ru make OH adsorption is stronger than that on pure Pt(111), which can lead to more difficult CO hydroxylation on Pt-Ru alloys with high Ru surface compositions. Thus, gradually increased barrier for CO hydroxylation are observed as increasing Ru surface compositions.

The rate-determining steps may be CH_2OH oxidation into CHOH intermediate via C-H bond cleavage and CO further oxidation into CO_2 through hydroxylation due to their almost identical and relatively higher activation barriers than other elementary steps on pure Pt(111) surface. CH_3OH oxidation rate only is determined by CO further oxidation into CO_2 after alloying of Pt with Ru since the barrier for CH_2OH oxidation into CHOH intermediate is significantly reduced (See Table 1). Notably, the lowest barrier of *ca*. 0.15 eV can be obtained when surface composition of Ru is *ca*. 50%. Simultaneously, we also observed that intermediates CHOH and COH formations have the lowest barriers when surface composition of Ru is *ca*. 50%. Thus, it can be speculated that the optimal Ru surface composition may be *ca*. 50% for CH_3OH oxidation on Pt-Ru alloys. Although CO further oxidation into CO_2 requires almost identical barrier when surface composition of Ru is *ca*. 50% with that on pure Pt(111) surface, the significantly stronger exothermic process for CO formation make CO_2 production be facile to occur (See Figure 2). When

surface composition of Ru is *ca*. 67%, the barriers for some elementary reaction steps are also reduced into the lowest values like formation pathways of CH_2OH and COH species and CH_3OH oxidation to produce CO intermediate has the strongest exothermicity (See Figure 3). However, it is noted that carbonaceous species, such as CH_3 that can poison the surface may be formed easily via C-O bond cleavage in CH_3OH with the notably decreased and surmountable barrier of *ca*. 0.38 eV at room temperature when surface composition of Ru is *ca*. 67%, suggesting that more than 50% Ru surface composition will be not favor of CH_3OH oxidation. Our present calculated Ru surface compositions of *ca*. 50% exhibits excellent consistency with the previous experimental studies. For example, the studies from Gasteiger et al., Weidner et al. and Wei et al showed that a *ca*. 50% of Ru surface composition can achieve the best electrocatalytic activity for CH_3OH oxidation and anti-CO poisoning ability,[37-40] confirming the reasonability of our present theoretical calculations to some degree.

Surface work function W is calculated in the presence of aqueous phase in order to determine origin of the enhanced electrocatalytic activity of Pt-Ru alloys towards CH_3OH oxidation in this paper. By definition, W is minimum energy required to extract one electron from surface to an infinite distance, which can be well calculated on the basis of DFT methods.[54, 55] The work function can be exactly calculated by equation:[56] $W = V_{vacuum} - E_F$, in which V_{vacuum} is vacuum level of pure Pt surface and Pt-Ru alloy systems and is defined to be mean electrostatic potential, and E_F is the Fermi level. The present calculated surface work function is 5.33, 5.28 and 5.12 eV on $Pt_2Ru(111)$, PtRu(111) and $PtRu_2(111)$, respectively, which are significantly lower than that of pure Pt(111) (5.50 eV), suggesting more electrons are transferred into various adsorbates on Pt-Ru alloys and facilitating CH_3OH oxidation. On this basis, we can approximately obtain the electrode potential (U) by referring the work function (Φ) of Pt-Ru alloy systems to the experimental work function of standard hydrogen electrode (SHE) on the basis of equation,[57, 58] $U = \Phi/e - 4.43$. The calculated electrode potential is 0.90, 0.85, and 0.69 V (*vs*. SHE), which is lower than that of pure Pt(111) surface (1.10 eV), implying that lower overpotentials are required for CH_3OH oxidation after alloying of Pt with Ru. Simultaneously, we also noted that the increasing Ru surface compositions can lead to the decreasing potentials. Thus, alloying of Pt with Ru will be favor of CH_3OH oxidation, explaining the above analysis of energetics. In fact, the previous experimental study on CH_3OH oxidation from Vielstich et al. also showed that alloying of Pt with Ru makes onset potentials decrease,[42] further confirming the accuracy of our present calculated results. However, more than 50% Ru surface compositions may go against CH_3OH oxidation. For example, C-O bond scission pathway of CH_3OH is facile to occur when surface composition of Ru is *ca*. 67%, which can lead to production of carbonaceous species that can poison surface active sites. Although our present calculated electrode potentials not always quantitatively accurate, the conclusions for effect of potentials on CH_3OH oxidation activity in trends is expected to be reasonably qualitatively correct.

3. Conclusions

In this paper, a deeper understanding on CH_3OH oxidation mechanisms on Pt-Ru alloys with different Ru surface compositions is provided by DFT-base theoretical studies. The present results show that indirect pathways and direct pathways may be able to parallelly occur on pure Pt surface, whereas only indirect pathways can occur after alloying of Pt with Ru. Simultaneously, alloying and surface compositions of Ru can change CH_3OH oxidation activity. The energetics of some elementary steps are notably decreased after alloying and the optimal surface composition of Ru is speculated be *ca*. 50%. Although the corresponding energetics are also notably reduced when surface composition of Ru is higher, carbonaceous species that can poison surface may be formed easily through initial C-O bond cleavage and key intermediate CO further oxidation into CO_2 product as rate-determining step become the most difficult to occur due to unfavorable H_2O dissociation to OH species, suggesting that more than 50% Ru surface composition will be not favor of CH_3OH oxidation. Our present calculated Ru surface compositions of *ca*. 50% exhibits excellent consistency with the previous experimental studies. The origin of enhanced catalytic activity of Pt-Ru alloys during CH_3OH oxidation is determined. The significantly decreased surface work functions after alloying Pt with Ru suggest more electrons are transferred into adsorbates compared with pure Pt(111) surface. The calculated electrode potential are lower than that of pure Pt(111) surface, implying that lower overpotentials are required for CH_3OH oxidation after alloying. Thus, alloying of Pt with Ru will be favor of CH_3OH oxidation. The excellent inconsistency with previous experimental study on decreased onset potentials after alloying further confirms the accuracy of our present calculated results.

Declarations

Funding

This work was supported by the Key Program of Education Department of Hunan Province (Grant No. 19A337); Hunan Provincial Natural Science Foundation of China (Grant No. 2018JJ2273); Key Program of Hunan University of Arts and Science (Grant No. 19ZD06); National Natural Science Foundation of China (Grant No. 21303048).

Conflicts of interest

The author has no relevant financial or non-financial interests to disclose.

Availability of data and material

Not applicable.

Code availability

Quantum ESPRESSO program package-http://www.quantum-espresso.org/;

XCRYSDEN graphical package-http://www.xcrysden.org/.

Author Contributions

Lihui Ou contributed to the study conception and design. Data collection and analysis were performed by Lihui Ou. The first draft of the manuscript was written by Lihui Ou.

References

1. A. Hamnett, Mechanism and Electrocatalysis in the Direct Methanol Fuel Cell, *Catal. Today*, 1997, **38**, 445-457.
2. U. A. Paulus, U. Endruschat, G. J. Feldmeyer, T. J. Schmidt, H. Bonnemann and R. J. Behm, New PtRu Alloy Colloids as Precursors for Fuel Cell Catalysts, *J. Catal.*, 2000, **195**, 383-393.
3. H. A. Gasteiger, N. Marković, P. N. Ross and E. J. Cairns, Carbon Monoxide Electrooxidation on Well-Characterized Platinum-Ruthenium Alloys, *J. Phys. Chem.*, 1994, **98**, 617-625.
4. M. Watanabe and S. Motoo, Electrocatalysis by Ad-Atoms: Part II. Enhancement of the Oxidation of Methanol on Platinum by Ruthenium Ad-Atoms, *J. Electroanal. Chem. Interfacial. Electrochem.*, 1975, **60**, 267-273.
5. H. A. Gasteiger, N. M. Marković and P. N Ross, H_2 and CO Electrooxidation on Well-Characterized Pt, Ru, and Pt-Ru. 1. Rotating Disk Electrode Studies of the Pure Gases Including Temperature Effects, *J. Phys. Chem.*, 1995, **99**, 8290-8301.
6. Y. P. Sun, L. Xing and K. Scott, Analysis of the Kinetics of Methanol Oxidation in a Porous Pt-Ru Anode, *J. Power Sources*, 2010, **195**, 1-10.
7. Q. Y. Lu, B. Yang, L. Zhuang and J. T. Lu, Anodic Activation of PtRu/C Catalysts for Methanol Oxidation, *J. Phys. Chem. B*, 2005, **109**, 1715-1722.
8. J. B. Xu, K. F. Hua, G. Z. Sun, C. Wang, X. Y. Lv and Y. J. Wang, Electrooxidation of Methanol on Carbon Nanotubes Supported Pt-Fe Alloy Electrode, *Electrochem. Commun.*, 2006, **8**, 982-986.
9. H. Uchida, H. Ozuka and M. Watanabe, Electrochemical Quartz Crystal Microbalance Analysis of CO-tolerance at Pt-Fe Alloy Electrodes, *Electrochim. Acta*, 2002, **47**, 3629-3636.
10. P. Hernández-Fernández, M. Montiel, P. Ocón, J. L. G. Fierro, H. Wang, H. D. Abruña and S. Rojas, Effect of Co in the Efficiency of the Methanol Electrooxidation Reaction on Carbon Supported Pt, *J. Power Sources*, 2010, **195**, 7959-7967.
11. D. J. Guo and S. K. Cui, Hollow PtCo Nanospheres Supported on Multi-Walled Carbon Nanotubes for Methanol Electrooxidation, *J. Colloid Interface Sci.*, 2009, **340**, 53-57.
12. X. W. Zhou, R. H. Zhang, Z. Y. Zhou and S. G. Sun, Preparation of PtNi Hollow Nanospheres for the Electrocatalytic Oxidation of Methanol, *J. Power Sources*, 2011, **196**, 5844-5848.
13. Q. Jiang, L. H. Jiang, H. Y. Hou, J. Qi, S. L. Wang and G. Q. Sun, Promoting Effect of Ni in PtNi Bimetallic Electrocatalysts for the Methanol Oxidation Reaction in Alkaline Media: Experimental and Density Functional Theory Studies, *J. Phys. Chem. C*, 2010, **114**, 19714-19722.

14. Q. Jiang, L. H. Jiang, S. L. Wang, J. Qi and J. Q. Sun, A highly Active PtNi/C Electrocatalyst for Methanol Electro-Oxidation in Alkaline Media, *Catal. Commun.*, 2010, **12**, 67-70.
15. I. T. Kim, H. K. Lee and J. Shim, Synthesis and Characterization of Pt-Pd Catalysts for Methanol Oxidation and Oxygen Reduction, *J. Nanosci. Nanotechnol.*, 2008, **8**, 5302-5305.
16. C. W. Xu, Y. Z. Su, L. L. Tan, Z. L. Liu, J. H. Zhang, S. Chen and S. P. Jiang, Electrodeposited PtCo and PtMn Electrocatalysts for Methanol and Ethanol Electrooxidation of Direct Alcohol Fuel Cells, *Electrochim. Acta*, 2009, **54**, 6322-6326.
17. A. O. Neto, R. R. Dias, M. Tusi, M. Linardi and E. V. Spinaće, Electro-Oxidation of Methanol and Ethanol using PtRu/C, PtSn/C and PtSnRu/C Electrocatalysts Prepared by an Alcohol-Reduction Process, *J. Power Sources*, 2007, **166**, 87-91.
18. Q. F. Yi, J. J. Zhang, A. C. Chen, X. P. Liu, G. R. Xu and Z. H. Zhou, Activity of a Novel Titanium-Supported Bimetallic PtSn/Ti Electrode for Electrocatalytic Oxidation of Formic Acid and Methanol, *J. Appl. Electrochem.*, 2008, **38**, 695-701.
19. W. W. He, X. C. Wu, J. B. Liu, K. Zhang, W. G. Chu, L. L. Feng, X. N. Hu, W. Y. Zhou and X. X. Xie, Pt-Guided Formation of Pt-Ag Alloy Nanoislands on Au Nanorods and Improved Methanol Electro-Oxidation, *J. Phys. Chem. C*, 2009, **113**, 10505-10510.
20. D. Zhao, Y. H. Wang, B. Yan and B. Q. Xu, Manipulation of Pt^Ag Nanostructures for Advanced Electrocatalyst, *J. Phys. Chem. C*, 2009, **113**, 1242-1250.
21. J. Luo, P. N. Njoki, Y. Lin, D. Mott, L. Y. Wang and C. J. Zhong, Characterization of Carbon-Supported AuPt Nanoparticles for Electrocatalytic Methanol Oxidation Reaction, *Langmuir*, 2006, **22**, 2892-2898.
22. J. Luo, M. M. Maye, N. N. Kariuki, L. Y. Wang, P. N. Njoki, Y. Lin, M. Schadt, H. R. Naslund and C. J. Zhong, Electrocatalytic Oxidation of Methanol: Carbon-Supported Gold-Platinum Nanoparticle Catalysts Prepared by Two-Phase Protocol, *Catal. Today*, 2005, **99**, 291-297.
23. C. X. Xu, R. Y. Wang, M. W. Chen, Y. Zhang and Y. Ding, Dealloying to Nanoporous Au/Pt Alloys and Their Structure Sensitive Electrocatalytic Properties, *Phys. Chem. Chem. Phys.*, 2010, 12, 239-246.
24. T. Y. Morante-Catacora, Y. Ishikawa and C. R. Cabrera, Sequential Electrodeposition of Mo at Pt and PtRu Methanol Oxidation Catalyst Particles on HOPG Surfaces, *J. Electroanal. Chem.*, 2008, **621**, 103-112.
25. F. Buatier de Mongeot, M. Scherer, B. Gleich, E. Kopatzki and R. J. Behm, CO Adsorption and Oxidation on Bimetallic Pt/Ru(0001) Surfaces – A Combined STM and TPD/TPR Study, *Surf. Sci.*, 1998, **411**, 249-262.
26. U. Käsberger and P. Jakob, Growth and Thermal Evolution of Submonolayer Pt Films on Ru(0001) Studied by STM, *Surf. Sci.*, 2003, **540**, 76-88.
27. P. Jakob and A. Schlapka, CO Adsorption on Epitaxially Grown Pt Layers on Ru(0001), *Surf. Sci.*, 2007, **601**, 3556-3568.

28. A. Schlapka, U. Käsberger, D. Menzel and P. Jakob, Vibrational Spectroscopy of CO used as a Local Probe to Study the Surface Morphology of Pt on Ru(0001) in the Submonolayer Regime, *Surf. Sci.*, 2002, **502**, 129-135.
29. A. Schlapka, M. Lischka, A. Groß, U. Käsberger and P. Jakob, Surface Strain versus Substrate Interaction in Heteroepitaxial Metal Layers: Pt on Ru(0001), *Phys. Rev. Lett.*, 2003, **91**, 016101.
30. P. Gazdzicki, S. Thussing and P. Jakob, Oxidation of Methanol on Oxygen Covered Pt_n/Ru(0001) Layers, *J. Phys. Chem. C*, 2011, **115**, 23013-23022.
31. L. H. Ou, Theoretical Insights into the Effect of Solvation and Sublayer Ru on Pt-Catalytic CH_3OH Oxidation Mechanisms in the Aqueous Phase, *J. Phys. Chem. C*, 2018, **122**, 14554-14565.
32. E. A. Franceschini, M. M. Bruno, F. J. Williams, F. A. Viva and H. R. Corti, High-Activity Mesoporous Pt/Ru Catalysts for Methanol Oxidation, *ACS Appl. Mater. Interfaces*, 2013, **5**, 10437-10444.
33. H. Hoster, T. Iwasita, H. Baumgärtner and W. Vielstich, Pt-Ru Model Catalysts for Anodic Methanol Oxidation: Influence of Structure and Composition on the Reactivity, *Phys. Chem. Chem. Phys.*, 2001, **3**, 337-346.
34. T. Iwasita, F. C. Nart and W. Vielstich, An FTIR Study of the Catalytic Activity of a 85: 15 Pt: Ru Alloy for Methanol Oxidation, *Ber. Bunsenges. Phys. Chem.*, 1990, **94**, 1030-1034.
35. T. Iwasita, H. Hoster, A. John-Anacker, W. F. Lin and W. Vielstich, Methanol Oxidation on PtRu Electrodes. Influence of Surface Structure and Pt–Ru Atom Distribution, *Langmuir*, 2000, **16**, 522-529.
36. P. N. Ross, The Science of Electrocatalysis on Bimetallic Surfaces, In *Electrocatalysis*, J. Lipkowski, P. N. Ross, Eds., Wiley-VCH: New York, 1998.
37. H. A. Gasteiger, N. Marković, P. N. Ross Jr and E. J. Cairns, Methanol Electrooxidation on Well-Characterized Pt-Ru alloys, *J. Phys. Chem.*, 1993, **97**, 12020-12029.
38. H. A. Gasteiger, N. Marković, P. N. Ross Jr and E. J. Cairns, Temperature-Dependent Methanol Electro-Oxidation on Well-Characterized Pt-Ru alloys, *J. Electrochem. Soc.*, 1994, **141**, 1795-1803.
39. T. R. Garrick, W. J. Diao, J. M. Tengco, E. A. Stach, S. D. Senanayake, D. A. Chen, J. R. Monnier and J. W. Weidner, The Effect of the Surface Composition of Ru-Pt Bimetallic Catalysts for Methanol Oxidation, *Electrochim. Acta*, 2016, **195**, 106-111.
40. Q. M. Wang, S. G. Chen, J. Jiang, J. X. Liu, J. H. Deng, X. Y. Ping and Z. D. Wei, Manipulating the Surface Composition of Pt-Ru Bimetallic Nanoparticles to control the Methanol Oxidation Reaction Pathway, *Chem. Commun.*, 2020, **56**, 2419-2422.
41. H. A. Gasteiger, N. Marković, P. N. Ross Jr and E. J. Cairns, Electro-Oxidation of Small Organic Molecules on Well-Characterized Pt-Ru Alloys, *Electrochim. Acta*, 1993, **39**, 1825-1832.
42. M. Krausa and W. Vielstich, Study of the Electrocatalytic Influence of Pt/Ru and Ru on the Oxidation of Residues of Small Organic Molecules, *J. Electroanal. Chem.*, 1994, **379**, 307-314.
43. A. Hamnett, Mechanism and Electrocatalysis in the Direct Methanol Fuel Cell, *Catal. Today*, 1997, **38**, 445-457.

44. R. Liu, H. Iddir, Q. Fan, G. Hou, A. Bo, K. L. Ley, E.S. Smotkin, Y. E. Sung, H. Kim, S. Thomas and A. Wieckowski, Potential-Dependent Infrared Absorption Spectroscopy of Adsorbed CO and X-Ray Photoelectron Spectroscopy of Arc-Melted Single-Phase Pt, PtRu, PtOs, PtRuOs, and Ru Electrodes, *J. Phys. Chem. B.*, 2000, **104**, 3518-3531.
45. P. Waszczuk, A. Wieckowski, P. Zelenay, S. Gottesfeld, C. Coutanceau, J. M. Leger and C. Lamy, Adsorption of CO Poison on Fuel Cell Nanoparticle Electrodes from Methanol Solutions: A Radioactive Labeling Study, *J. Electroanal. Chem.*, 2001, **511**, 55-64.
46. R. Nagao, D. A. Cantane, F. H. B. Lima and H. Varela, Influence of Anion Adsorption on the Parallel Reaction Pathways in the Oscillatory Electro-Oxidation of Methanol, *J. Phys. Chem. C*, 2013, **117**, 15098-15105.
47. V. S. Bagotzky, Y. B. Vassiliev and O. A. Khazova, Generalized Scheme of Chemisorption, Electrooxidation and Electroreduction of Simple Organic Compounds on Platinum Group Metals, *J. Electroanal. Interfacial Electrochem.*, 1977, **81**, 229-238.
48. R. Parsons and T. Vandernoot, The Oxidation of Small Organic Molecules: A Survey of Recent Fuel Cell Related Research, *J. Electroanal. Interfacial Electrochem.*, 1988, **257**, 9-45.
49. J. Greeley and M. Mavrikakis, Competitive Paths for Methanol Decomposition on Pt(111), *J. Am. Chem. Soc.*, 2004, **126**, 3910-3919.
50. J. Greeley and M. Mavrikakis, A First-Principles Study of Methanol Decomposition on Pt(111), *J. Am. Chem. Soc.*, 2002, **124**, 7193-7201.
51. D. Cao, G. Q. Lu, S. A. Wasileski and M. Neurock, Mechanisms of Methanol Decomposition on Platinum: A Combined Experimental and ab Initio Approach, *J. Phys. Chem. B*, 2005, **109**, 11622-11633.
52. T. Mattsson and S. Paddison, Methanol at the Water-Platinum Interface Studied by Ab Initio Molecular Dynamics, *Surf. Sci.*, 2003, **544**, L697-L702.
53. Y. Okamoto, O. Sugino, Y. Mochizuki, T. Ikeshoji and Y. Morikawa, Comparative Study of Dehydrogenation of Methanol at Pt(111)/Water and Pt(111)/Vacuum Interfaces, *Chem. Phys. Lett.*, 2003, **377**, 236-242.
54. M. Methfessel, D. Hennig and M. Scheffler, Trends of the Surface Relaxations, Surface Energies, and Work Functions of the 4*d* Transition Metals, *Phys. Rev. B*, 1992, **46**, 4816-4829.
55. H. L. Skriver and N. M. Rosengaard, Surface Energy and Work Function of Elemental Metals, *Phys. Rev. B*, 1992, **46**, 7157-7168.
56. N. D. Lang and W. Kohn, Theory of Metal Surfaces: Work Function, *Phys. Rev. B*, 1971, **3**, 1215-1222.
57. J. D. Goodpaster, A.T. Bell and M. Head-Gordon, Identification of Possible Pathways for C-C Bond Formation during Electrochemical Reduction of CO_2: New Theoretical Insights from an Improved Electrochemical Model, *J. Phys. Chem. Lett.*, 2016, **7**, 1471-1477.
58. Challenges in Modelling Electrochemical Reaction Energetics with Polarizable Continuum Models, *ACS Catal.*, 2019, **9**, 920-931.

Figures

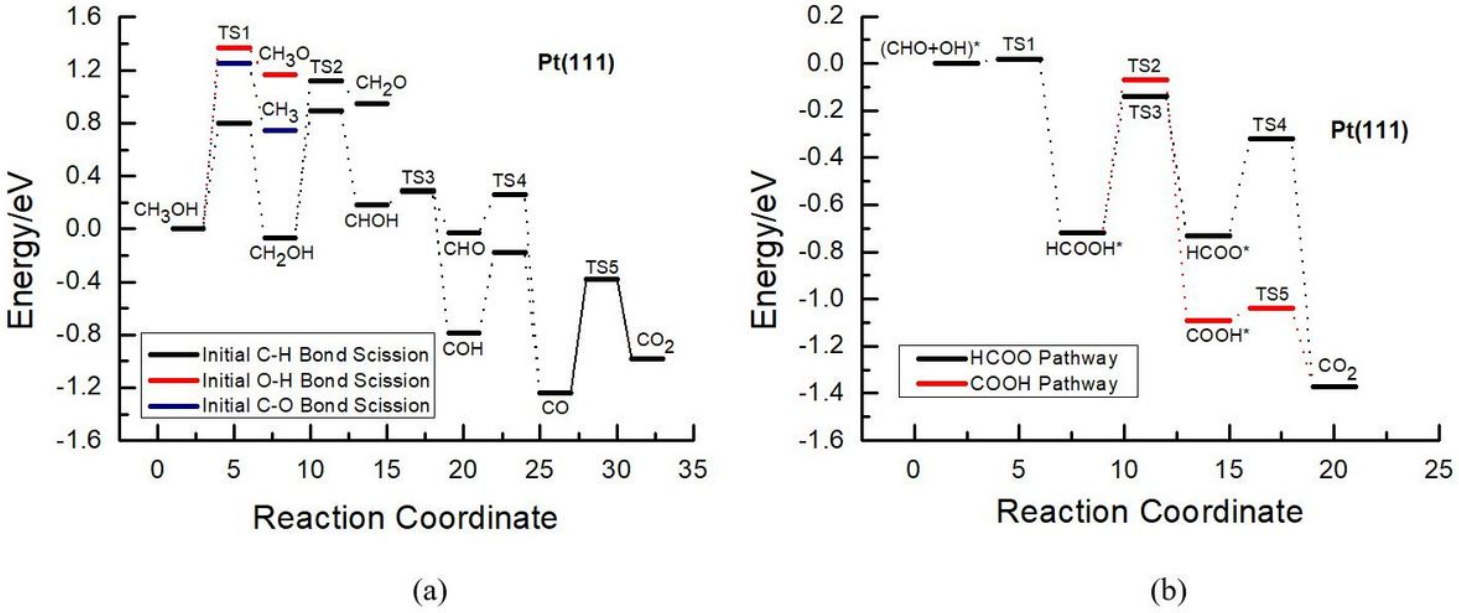

Figure 1

Overall energy pathway diagram for (a) indirect pathways of CH_3OH oxidation to form CO_2 and direct pathways of CH_3OH oxidation started CHO hydroxylation in aqueous phase on pure Pt(111) surface.[31]

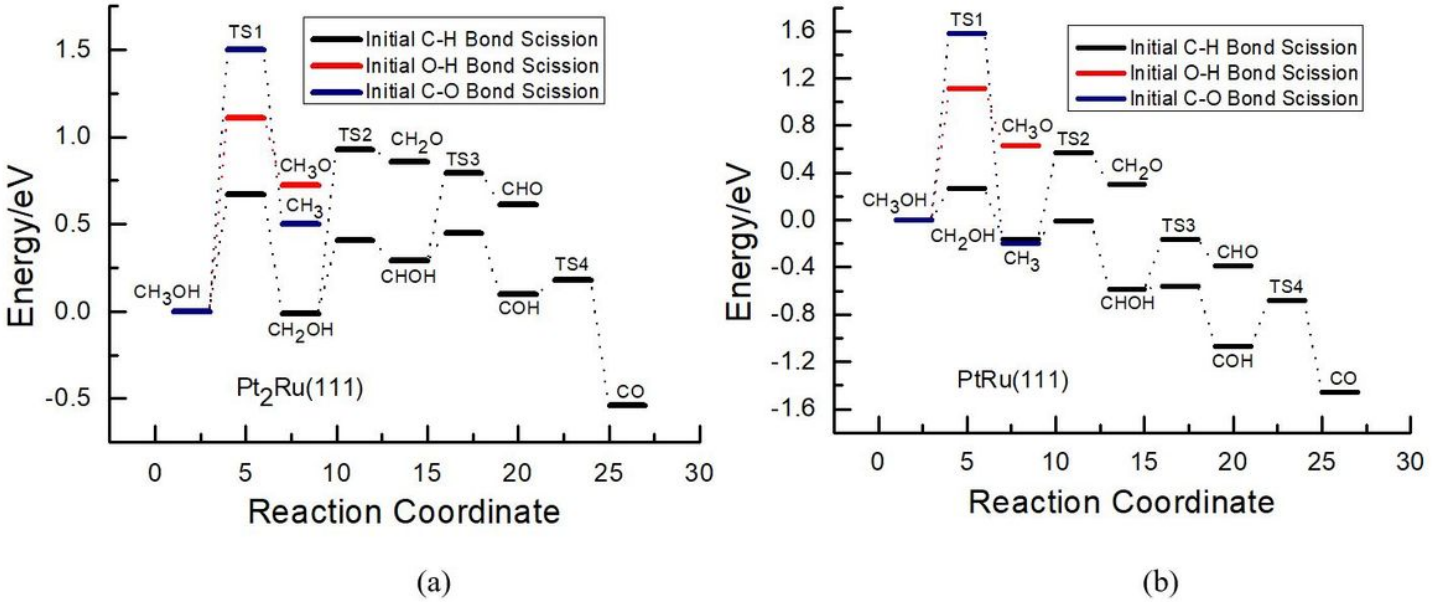

Figure 2

Overall energy pathway diagram for CH_3OH electrooxidation to form CO intermediate initial C-H, O-H and C-O bond cleavage on (a) $Pt_2Ru(111)$ and (b) PtRu(111) in aqueous phase.

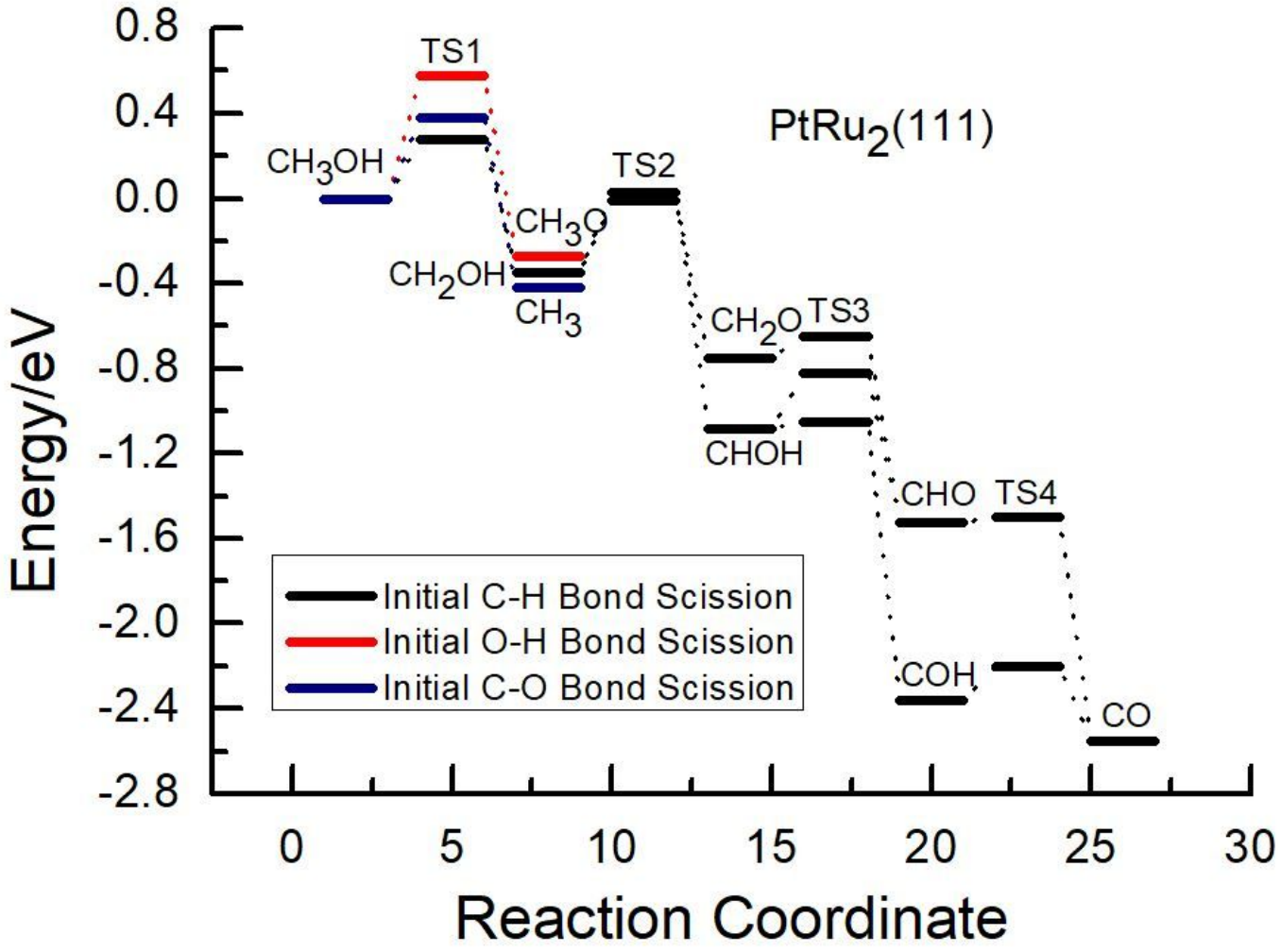

Figure 3

Overall energy pathway diagram for CH_3OH electrooxidation to form CO intermediate initial C-H, O-H and C-O bond cleavage on $PtRu_2(111)$ in aqueous phase.

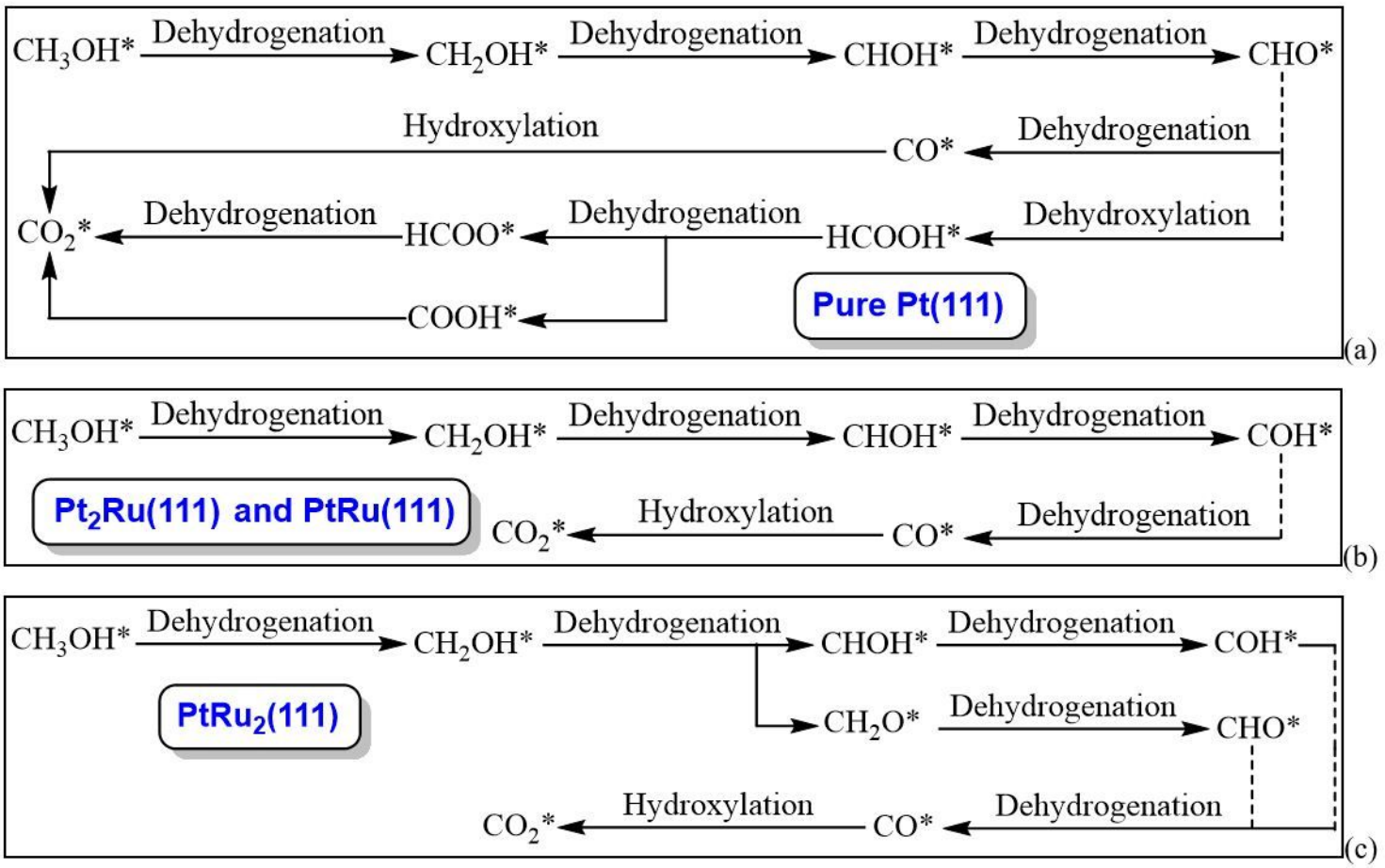

Figure 4

The optimal CH_3OH oxidation pathways to produce CO intermediate on (a) pure Pt(111) surface, (b) $Pt_2Ru(111)$ and PtRu(111) and (c) $PtRu_2(111)$.

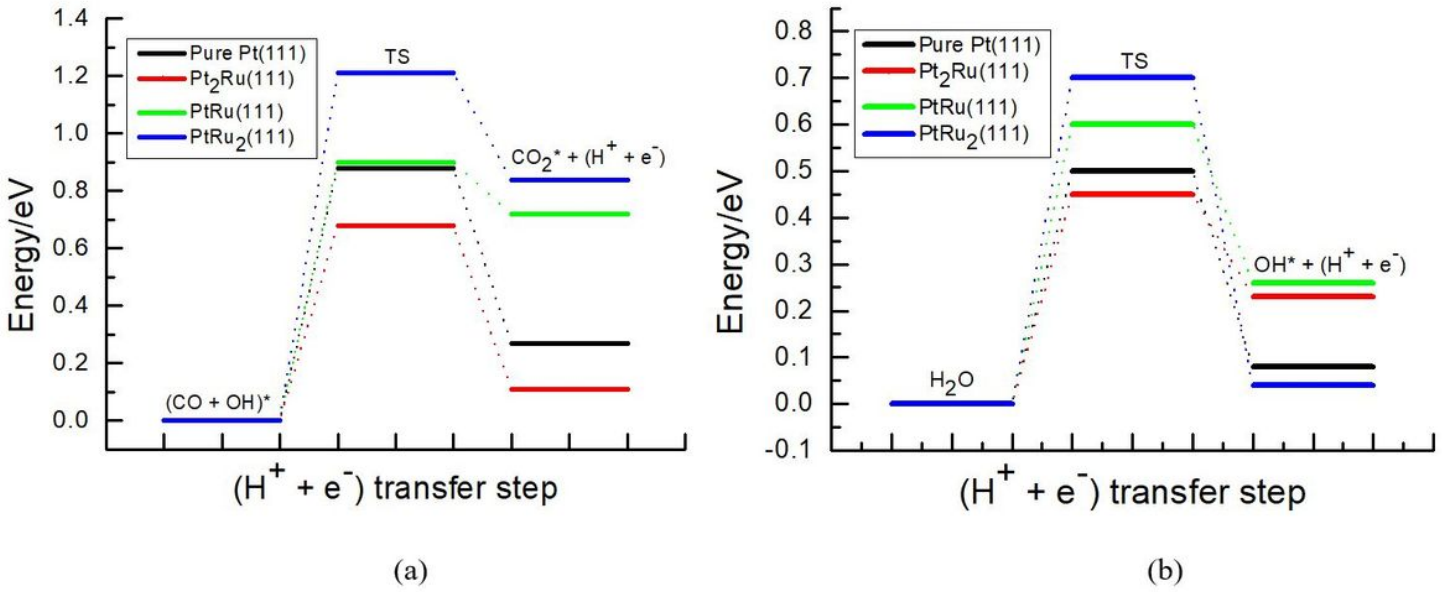

Figure 5

Energy pathway diagram for (a) CO oxidation into CO_2 product and (b) H_2O dissociation into adsorbed OH on pure Pt(111), $Pt_2Ru(111)$, PtRu(111) and $PtRu_2(111)$ in aqueous phase.

Supplementary Files

This is a list of supplementary files associated with this preprint. Click to download.

- Abstractgraphic.doc
- SupportingInformationCH3OHOxidation.doc